International Journal of Pharmaceutics, 8 (1981) 45–62

KINETICS AND MECHANISMS OF AQUEOUS DEGRADATION OF THE ANTICANCER AGENT, INDICINE N-OXIDE

JOSEPH B. D'SILVA and ROBERT E. NOTARI *

College of Pharmacy, The Ohio State University, 500 W. 12th Avenue, Columbus, Ohio 43210 (U.S.A.)

(Received October 6th, 1980)
(Revised version received January 12th, 1981)
(Accepted January 14th, 1981)

SUMMARY

The aqueous degradation of indicine N-oxide, an unsaturated pyrrolizidine alkaloid ester undergoing clinical testing as an anticancer agent, was studied as a function of pH, buffers and temperature using a colorimetric TLC assay. Isolation and identification of reaction products demonstrated that ester hydrolysis yielding retronecine N-oxide and trachelanthic acid represents the primary alkaline degradation pathway. No loss of indicine N-oxide could be detected in acidic conditions nor could any contribution from uncatalyzed water attack be observed. The pH–rate profiles in alkaline pH at several temperatures indicate that apparent first-order rate-constants may be defined as $k_{obs} = k_{OH^-}[OH^-]$. The energy of activation (16.1 kcal/mol) is relatively high for the aqueous hydrolysis of an ester. The kinetics of hydrolysis are discussed relative to other esters and both steric hindrance and β-hydroxyl intramolecular catalysis are proposed. NMR and mass spectral details for indicine N-oxide, retronecine N-oxide and trachelanthic acid are reported.

INTRODUCTION

Several pyrrolizidine alkaloid derivatives possess anti-tumor activity (Culvenor, 1968; Kugelman et al., 1976; Kupchan and Suffness, 1967). Indicine N-oxide (I), found in *Heliotropium indicum* Linn (Boraginaceae) (Kugelman et al., 1976), is undergoing clinical trials (Ames and Powis, 1978). Its aqueous stability has not been reported.

* To whom correspondence should be addressed.

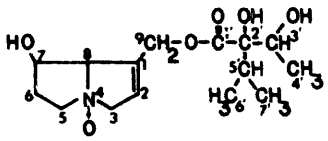

I

Bull et al. (1968) compared the degradation rates of several pyrrolizidine alkaloid esters in 0.5 N aqueous or hydroalcoholic sodium hydroxide at room temperature. The increased rate of hydrolysis of indicine in comparison to that of its 3′-methoxy derivative suggested β-hydroxy participation presumably via hydrogen bonding. Similar intramolecular catalysis would be anticipated for indicine N-oxide, an ester of retronecine N-oxide and trachelanthic acid.

This paper reports the kinetics and mechanisms of aqueous degradation of indicine N-oxide as a function of pH, buffers and temperature. Indicine N-oxide concentrations were determined using a previously developed stability-indicating assay (D'Silva and Notari, 1980) wherein reaction samples are quenched by adjusting the pH to 2–4.5. Indicine N-oxide is separated from the reaction mixture by thin-layer chromatography on silica-coated aluminum sheets. The silica containing the indicine N-oxide is treated with diglyme and acetic anhydride at 100°C. The resultant pyrrole is coupled with *p*-dimethylaminobenzaldehyde to produce a color and the absorbance is monitored at 566 nm.

Ester hydrolysis was found to be the sole degradation pathway under all conditions in this study. Isolation and identification of hydrolysis products provided retronecine N-oxide and (–)-trachelanthic acid. Indicine N-oxide was observed to be susceptible to specific hydroxyl-ion catalysis and to be stable in acid. Comparison of indicine N-oxide kinetics to those reported for related analogs (Bull et al., 1968) confirms that the 3′-hydroxyl accelerates the hydrolysis rate.

MATERIALS AND METHODS

Materials

Indicine N-oxide was purified by recrystallization from methanol–acetone (Kugelman et al., 1976). All chemicals were analytical reagent grade obtained from the sources previously reported (D'Silva and Notari, 1980). Buffers were prepared with carbon dioxide-free double-distilled water. NMR spectra were recorded in deuterium oxide, 99.8% atom D (Aldrich, Wisc., U.S.A.) or $CdCl_3$, 99.8% atom D (Aldrich, Wisc., U.S.A.).

Instrumentation

Absorbance was measured using a Gilford 250 spectrophotometer. Proton spectra were recorded on a Bruker HX-90E spectrometer and carbon-13 spectra were obtained using a Bruker WP-80 spectrometer both in the pulse mode. IR spectra were recorded using a Beckman IR 4230 spectrophotometer. A high pH combination electrode (A.H. Thomas, Philadelphia, Pa., U.S.A.) together with a Corning model 12 pH meter were used. Mass spectra were recorded on a DuPont 21-491 mass spectrometer at 70 eV. Optical rotation values were recorded using a Perkin-Elmer 241 polarimeter.

TABLE 1

REACTION CONDITIONS AND APPARENT FIRST-ORDER RATE-CONSTANTS FOR HYDROLYSIS OF INDICINE N-OXIDE [a]

No.	Temperature (°C)	Reaction medium	pH	μ	k_1 (h^{-1})
1	30	0.08 N NaOH	12.60 [b]	0.08	1.06
2		0.10 N NaOH	12.69 [b]	0.10	1.30
3		0.15 N NaOH	12.85 [b]	0.15.	1.79
4		0.20 N NaOH	12.98 [b]	0.20	2.52
5		0.25 N NaOH	13.06 [b]	0.25	3.09
6		0.20 N NaOH + 0.81 M NaCl	12.93 [c]	1.01	2.17
7		0.535 M Na_3PO_4	12.20	2.12	0.463
8		0.1 N NaOH + 0.302 sodium glycine	12.70	0.40	1.25
9		0.1 N NaOH + 0.0513 Na_3PO_4	12.77	0.35	1.39
10	40	0.07 N NaOH	12.27 [b]	0.07	2.34
11		0.04 N NaOH	12.04 [b]	0.04	1.43
12		0.12 M Na_3PO_4 + 0.0798 M Na_2HPO_4 pH adjusted with NaOH	11.52	0.66	0.553
13		0.704 M sodium glycine pH adjusted with HCl	10.50	1.3	0.034
15	60	0.12 M Na_3PO_4 0.0798 M Na_2HPO_4	11.32	0.96	5.34
16		0.4 M sodium glycine + 0.320 M NaCl, pH adjusted with HCl	10.00	0.87	0.181
17		0.702 M sodium glycine, pH adjusted with HCl	10.02	1.14	0.204
18		0.6 M sodium glycine pH adjusted with HCl	8.90	1.13	0.0201
19	90	0.601 M sodium glycine pH adjusted with HCl	8.28	1.18	0.272
20		0.115 M NaH_2PO_4 + 0.156 Na_2HPO_4 + 0.422 NaCl	6.58	1.00	0.00697
21		0.267 M NaH_2PO_4 + 0.0887 Na_2HPO_4 + 0.489 NaCl	6.10	1.02	0.00346

[a] Reaction solutions 1 through 6 and 8 and 9 contained 7×10^{-3} M indicine N-oxide while the rest of the solutions contained 3×10^{-3} M indicine N-oxide.

[b] Calculated from $[OH^-]$ using K_W and $\gamma_\pm$ from Harned and Owen (1958).

[c] Calculated from $[OH^-]$ using K_W and $\gamma_\pm$ from: (1) Harned and Owen (1958); and (2) Harned and Cook (1937). All other pH values were experimentally determined.

Kinetics of indicine N-oxide hydrolysis in sodium hydroxide or buffered solutions

All reaction samples were assayed by a previously reported stability indicating method (D'Silva and Notari, 1980) which is applicable to indicine N-oxide reaction concentrations in the range of $\sim 3 \times 10^{-3}$ M to $\sim 8 \times 10^{-3}$ M. Aliquots (30–70 μl) were withdrawn from reaction solutions at constant temperature as a function of time and quenched with 5–10 μl of formic acid (0.15–19 M) to adjust the pH to 2–4 and assayed. Apparent first-order hydrolysis conditions are given in Table 1.

Buffer concentrations were of sufficient capacity to maintain the pH during trachelanthic acid formation. In general, buffered reactions were maintained at an ionic strength (μ) close to one. In a few more concentrated buffers this was not possible (Table 1). However, the hydrolysis rate was found to be independent of μ within the limits studied.

Second-order reaction conditions are given in Table 2. Ten-μl aliquots were withdrawn as a function of time, quenched with 20 μl of 0.2 M formic acid and assayed. The decrease in indicine N-oxide concentration with time was used to calculate the bimolecular rate-constants.

Stability testing of indicine N-oxide under acidic conditions

Both chromatography and polarimetry were used to evaluate the stability of indicine N-oxide in acid. Solutions containing 0.03 M indicine N-oxide in 0.5 N HCl were heated at 70°C for 21 h, cooled and 20-μl aliquots were spotted adjacent to authentic indicine N-oxide samples on TLC sheets coated with silica gel 60 F-254 (Merck). These were developed for 12 cm with ether–ethanol–water–ammonia solution (5 : 4 : 1 : 1), air-dried and visualized by spraying with a sulfuric acid–ether (1 : 4) mixture and heated. Before and after the reaction, aliquots were diluted with phosphate buffer to provide 0.015 M indicine N-oxide rotations at pH 6.5. The optical solution was determined at

TABLE 2

INITIAL CONCENTRATIONS (M/liter) OF INDICINE N-OXIDE [C_0] AND SODIUM HYDROXIDE [NaOH] AND OBSERVED BIMOLECULAR RATE-CONSTANTS [a]

Temperature (°C)	$[C_0] \times 10^2$	$[NaOH] \times 10^2$	k_2 (l/M-h)
22	4.15	7.86	5.27
30	4.06	7.81	10.8
	4.06	7.86	12.6
	4.02	7.86	11.7
	2.00	5.93	12.9
	1.51	4.72	12.6
40	5.96	7.86	24.1
	3.99	7.86	27.4
	3.98	7.83	27.9
50	3.99	7.86	57.6
	3.02	7.86	59.4

[a] Calculated from Eqn. 3.

24°C using the green mercury line (546 nm). Buffer solutions of pH 3.0, 4.1, and 5.2 (90°C) were prepared containing ~0.2 M citric acid and NaOH. Reaction solutions of indicine N-oxide (~2×10^{-3} M) were prepared using these buffers and heated at 90°C for 31 h. The solutions were cooled and 5-μl aliquots were directly chromatographed as described above for 0.5 HCl reactions.

Isolation and identification of degradation products of indicine N-oxide in sodium hydroxide solutions

In the following procedure chromatographic identification was conducted as described in the previous section. Thin-layer chromatograms from reaction solutions listed in Tables 1 and 2 showed only the reactant and two degradation products. To verify this, 3 developing solvents were employed in the chromatographic separations. Indicine N-oxide (7 mg) was dissolved in 1 ml of 0.1 N NaOH and heated at 40°C for 12 h. Aliquots of the reaction solution were chromatographed using the same TLC procedure as above but also using the following solvent systems to develop the chromatograms: methanol–acetone (18 : 1) and *n*-butanol–acetic acid–water (5 : 1 : 1). Again, only two degradation products were visualized on all 3 chromatograms.

To test the acid stability of the degradation products, an aliquot of reaction mixture was adjusted to pH = 1 using 1 N HCl and heated at 40°C for 7 h. The pH was readjusted to 11 using 1 N NaOH and the solution analyzed by TLC using all 3 solvent systems. The products were found to be stable.

The hydrolysis products of indicine in 2.0 N NaOH at 100°C for 2 h were shown to be retronecine and a diastereomer of trachelanthic acid (Mattocks et al., 1961). Therefore, the hydrolysis of indicine N-oxide in aqueous sodium hydroxide was expected to produce the products shown in Scheme I, although the formation of other products such as pyr-

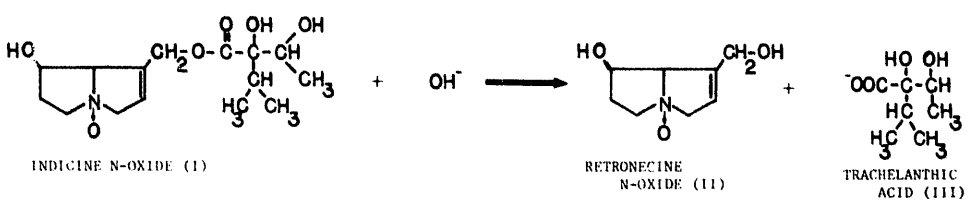

Scheme I

roles due to the presence of the N-oxide could not be ruled out a priori. The chromatographic analysis of the hydrolysis solutions of indicine N-oxide indicated the presence of retronecine N-oxide and trachelanthic acid and the following procedure was developed to isolate the products.

Indicine N-oxide (0.35 g) was dissolved in 45 ml of 0.1 N NaOH. The solution was heated at 40°C for 12 h, cooled and tested by TLC to demonstrate total degradation of indicine N-oxide. The mixture was diluted with 100 ml of water, the pH adjusted to 1.5 using 1 N HCl and the volume made up to 200 ml with water. This was continuously extracted with 150 ml of ether for 36 h. The ether extract was separated from the aqueous raffinate and evaporated to dryness under vacuum in a rotary evaporator. The resulting white crystalline product (148 mg after drying over phosphorus pentoxide) had

a melting point range of 86–86.5°C. After recrystallization from benzene–petroleum ether (ether b.p. 35–60°C), the product had a m.p. of 91.8°C. Proton and carbon-13 spectra in $CdCl_3$ using TMS as internal standard, IR and mass spectra were obtained. The optical rotation of a 20.97 mg/ml solution of this material in carbon dioxide-free water was determined at 22.5°C using the sodium D-line of visible light. The solution was made up to 10 ml with carbon dioxide-free water at 22.5°C and 0.2 ml of 0.4 N HCl was added. The mixture was titrated with 0.45 N NaOH added in 5-μl increments and the pH was recorded after each addition. The titration was stopped at pH 11.4 and the mixture was then back-titrated with 0.4 N HCl to pH 1.96. In both cases the pK_a was calculated to be 3.77 using second derivative plots ($\Delta pH/\Delta V$ vs V where V is the volume of titrant added) to determine the pH of half-neutralization.

The pH of the aqueous raffinate was adjusted to 6.62 using 1.0 N NaOH, and freeze-dried to obtain a white powder which contained a considerable amount of sodium chloride. The powder was thoroughly mixed with 40 ml of anhydrous methanol and filtered. The filtrate was placed in a freezer to reprecipitate any dissolved NaCl, filtered cold and evaporated. The methanol extraction was repeated until an aliquot of extract gave only a very faint positive chloride test using $AgNO_3$ and 0.5 N HNO_3. The solution was evaporated to obtain a pale yellow powder which was dissolved in 9 ml of methanol. Two ml of acetone were added and the solution was evaporated. Pale yellow rosette crystals (114 mg melting at 193°C with decomposition) were obtained. Mass spectra and proton and carbon-13 spectra (in D_2O) were obtained. DSS was used as an internal standard in proton spectra and dioxane was used as an external standard in carbon-13 spectra.

pK_a determination of indicine N-oxide

Indicine N-oxide (35 mg) was dissolved in 10 ml of carbon dioxide-free water at 22.5°C. An aliquot of HCl was added and the mixture was titrated as described above with 0.45 N NaOH to determine the $pK_a = 4.35$.

RESULTS AND DISCUSSION

Rate-constants in sodium hydroxide and buffered solutions

Good first-order plots were obtained when experimental data from reaction solutions described in Table 1 were graphed according to:

$$\ln A = \ln A_0 - k_1 t \quad (1)$$

where A is the 566 nm absorbance due to unreacted indicine N-oxide at time t, A_0 is the initial absorbance and A_∞ is zero. A plot of k_1 versus hydroxide-ion activity (a_{OH^-}) at 30°C (reactions 1–5, Table 1) was linear with slope 17.9 l/M-h and negligible intercept ($r = 0.9990$) in accordance with:

$$k_1 = k_{a_{OH^-}}(a_{OH^-}) \quad (2)$$

where $k_{a_{OH^-}}$ is the bimolecular rate-constant for the hydrolysis of indicine N-oxide. The (a_{OH^-}) values were calculated from either the known value for $[OH^-]$ or the experimen-

tally determined pH values by using the K_w and $\gamma_\pm$ values reported by Harned and Owen (1958).

In order to ensure that ionic strength and buffer effects were insignificant in this pH region, the rate-constants for reactions 6–9 (Table 1) were also tested using Eqn. 2. There was no significant difference in the regression with or without these values. Thus, the increase in μ (reactions 6 and 7), or addition of buffer components (reactions 7–9) did not affect the rate provided that the activity of the hydroxide ion is corrected for μ. Likewise, the effect of varying buffer concentration at a given pH was studied using 0.400 and 0.702 M sodium glycine adjusted to pH 10.0 with HCl. The rate-constants were within 10% of each other (reactions 16 and 17, Table 1).

Second-order rate-constants were calculated from the slopes of plots based on:

$$\frac{1}{(a-b)} \cdot \ln \frac{b(a-x)}{a(b-x)} = k_2 t \qquad (3)$$

where a is the initial concentration of NaOH, b is the initial concentration of indicine N-oxide, x is the change in indicine N-oxide concentration at time, t, and k_2 is the second-order hydrolysis rate-constant, in units derived from the concentration of NaOH and indicine N-oxide. Typical plots are shown in Fig. 1 and rate-constants are listed in Table 2. The average bimolecular rate-constant at 30°C (12.1 l/M-h) when multiplied by the NaOH concentrations predicts k_1 values in good agreement with those reported in Table 1.

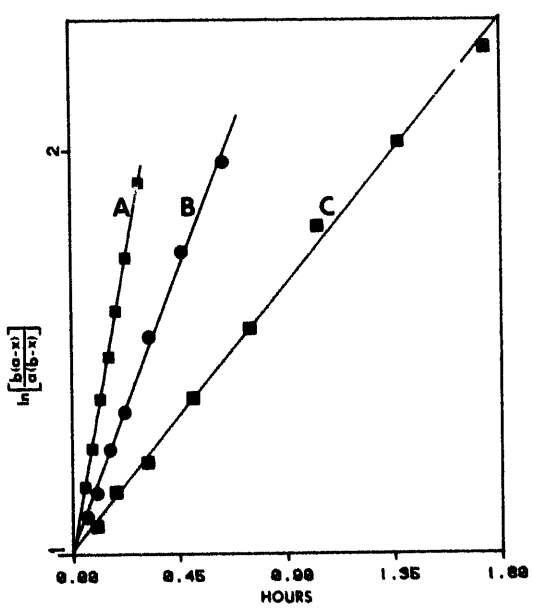

Fig. 1. Semi-ln plots based on Eqn. 3 to determine the bimolecular rate-constant, k_2 = slope/(a − b), for hydrolysis of ~0.04 M indicine N-oxide in ~0.08 M at (A) 50°C, (B) 40°C and (C) 30°C.

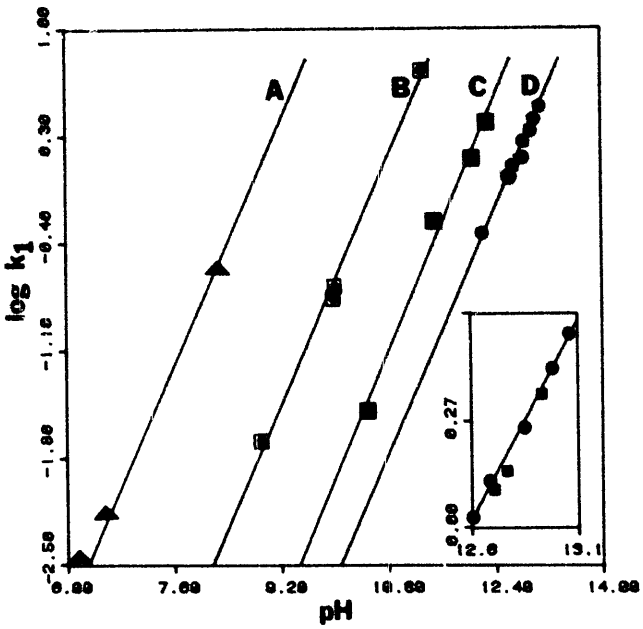

Fig. 2. Semi-log plots of the first-order rate-constants (k_1) for indicine N-oxide hydrolysis as a function of pH at (A) 90°C, (B) 60°C, (C) 40°C and (D) 30°C where lines are drawn to a slope of 1.0 in agreement with Eqn. 4. Insert shows expanded scale for (D) at pH 12.6–13.1 to illustrate lack of difference between buffered (■) and unbuffered (●) rate-constants.

pH–rate profile

The log transformation of Eqn. 2 is:

$$\log k_1 = \log k_{a_{OH^-}} + pH \tag{4}$$

Fig. 2 presents the log k_1 vs pH plots for the data in Table 1. The slopes of the lines agree with the theoretical value of 1, thus showing that under these conditions hydrolysis is due primarily to attack by hydroxide ion with no significant uncatalyzed water attack. In the case of 30°C data, the rate-constants using unbuffered hydroxide solutions (solutions 1–5, Table 1) were employed to establish the linear regression line (Fig. 2). The rate-constants obtained using buffered solutions (6–9, Table 1) are shown to be on this line demonstrating that changes in μ or buffer components did not significantly alter the pH-profile.

Stability of indicine N-oxide under acidic conditions

The indicine N-oxide pK_a (found to be 4.35 at 22.5°C) is consistent with the reported value of 4.25 at 23°C (McCornish et al., 1980). The acid stability of the protonated form was demonstrated by the lack of chromatographic evidence for degradation when indicine N-oxide was heated in 0.5 N HCl at 70°C. Epimerization is not likely under these conditions since the specific rotation ($[\alpha]^{24°C}_{546nm}$ = +24) was unchanged. Further evidence of acid stability of both the protonated and non-protonated forms of indicine N-oxide was

obtained by heating at pH 2.99, 4.06 and 5.17 in citrate buffers under conditions sufficient to cause 10% degradation at pH 6 and at concentrations sufficient for products to be visible. No degradation products were observed on the chromatograms.

Isolation and characterization of degradation products of indicine N-oxide in sodium hydroxide solutions

Chromatographic analyses of aqueous hydrolyzed solutions of indicine N-oxide showed only two degradation products identified as (–)-trachelanthic acid and retronecine N-oxide ($R_f = 0.53$ and $R_f = 0.27$ in the ethanol–ether–water–ammonia system). The white crystalline product from the ether extract of the acidified solution was (–)-trachelanthic acid, $pK_a = 3.77$ (±0.05), 22.5°C; m.p. 91.8°C; $[\alpha]_D^{22.5°C} - 3.34$. (Literature values: m.p. 90–91°C, $[\alpha]_D^{22} - 2.4$ in water found by Kochetkov et al., 1969 and m.p. 89°C, $[\alpha]_D^{25} - 3.4$ in water found by Adams and Van Duuren, 1952.) The average purity of the sample based on titration was 97.3% (±2.7%). The IR spectrum of trachelanthic acid in $CHCl_3$ solution showed a broad band (3600–2600 cm^{-1}) attributed to the carboxylic acid and the hydrogen-bonded hydroxyl group (II). A sharp peak at 3500 cm^{-1} was assigned to hydroxyl group stretching, and multiple peaks at 1725 and 1760 cm^{-1} to the hydrogen-bonded carbonyl group.

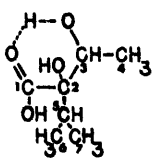

II

The proton spectra in $CdCl_3$ displayed a pair of doublets at 0.94 ppm (J = 2.86 Hz, 3H) and 1.01 ppm (J = 2.86 Hz, 3H), assigned to the methyl protons at C_6 and C_7. The appearance of separate doublets could be due to the added deshielding of one of the methyl groups by the anisotropic deshielding cone of the carbonyl oxygen. A doublet at 1.27 ppm (J = 6.36 Hz, 3H) was attributed to the C_4 methyl group, a quartet centered at 4.2 ppm (1H) to the C_4 proton, and the C_5 proton assigned to a 5 peak multiplet centered at 2.14 ppm (1H). The exchangable protons from the carboxylic acid and hydroxyl groups coalesce to produce a broad singlet at 3.1 ppm. The carbon-13 spectrum of trachelanthic acid in $CdCl_3$ showed 6 peaks and the assignments are as follows; δ 16.65 (C4), δ 16.89 (C6, C7), δ 32.89 (C5), δ 69.82 (C3), δ 82.85 (C2), and δ 177.47 (C1).

Major mass spectral degradation fragments of trachelanthic acid are shown in Scheme II. A molecular ion (m/e 162) was formed with a very low abundance. Major degradation reactions were dehydrations (m/e 162 → 144, m/e 118 → 100, m/e 103 → 85) and loss of carbon dioxide (m/e 162 → 118). Other pathways included loss of methyl and hydrogen radicals. At high inlet concentrations a chemical ionization mass spectrum of trachelanthic acid was recorded, presumably due to protonation by charged species produced in the spectrometer. The degradation pathways remained generally similar to the electron impact spectrum and are shown in Scheme II. Two major differences between the spectra were the production of a strong quasi-molecular ion at m/e 163, and the base peak shifting from m/e 71 to m/e 103.

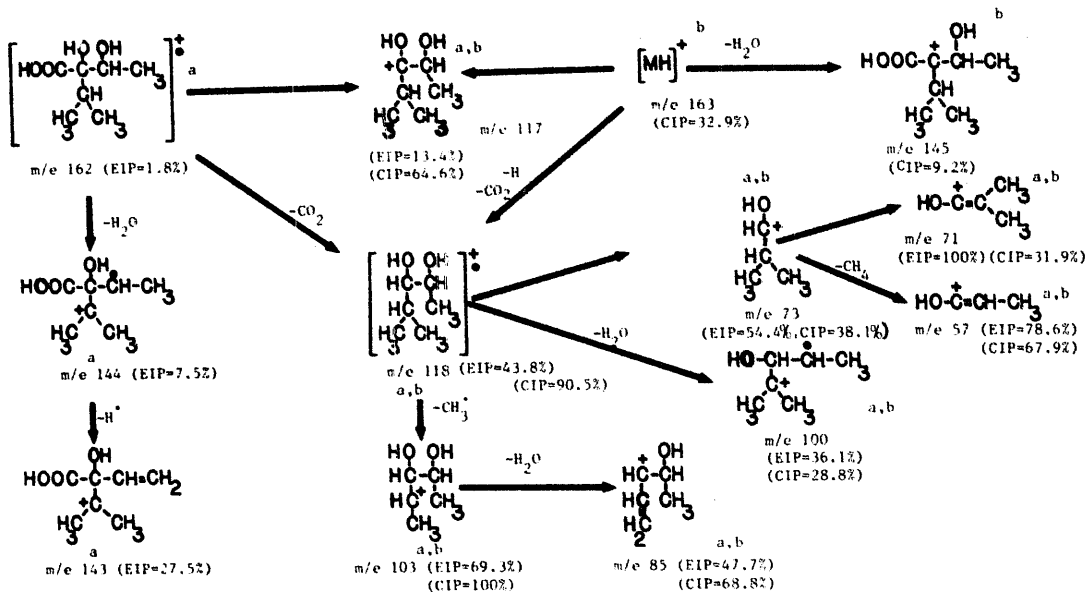

Scheme II

Retronecine N-oxide, m.p. 193°C with decomposition (literature value, ~200°C with decomposition; in Bull et al., 1968), was isolated from the raffinate. It gave a strong positive test for N-oxide derivatives of unsaturated pyrrolizidine alkaloids when treated with acetic anhydride and heat followed by *p*-dimethylaminobenzaldehyde according to the method of Mattocks (1967). The proton spectrum (Fig. 3) of retronecine N-oxide (III) measured at 90 MHz in D_2O was complicated by numerous coupling interactions between

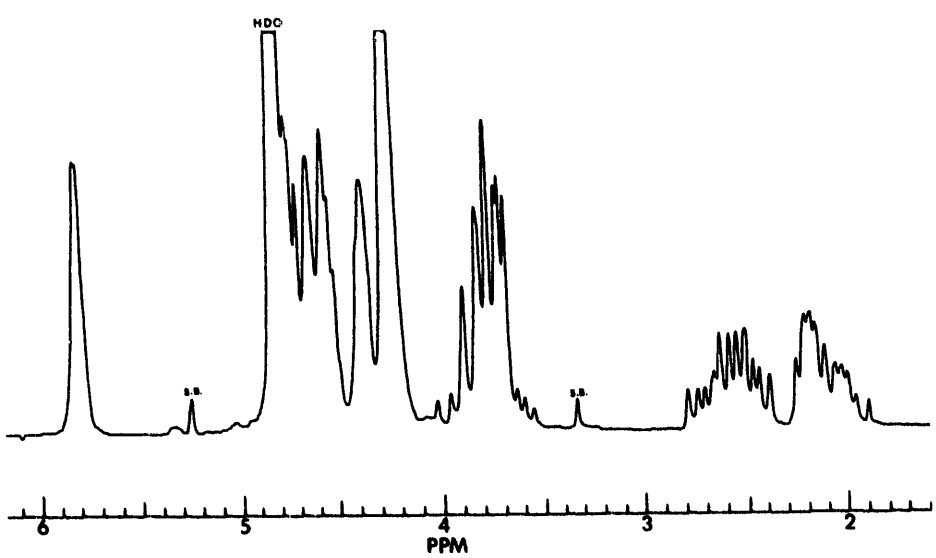

Fig. 3. PNMR spectrum of retronecine N-oxide measured at 90 Mc/s in D_2O.

the various geminal protons, and the assignments are as follows:

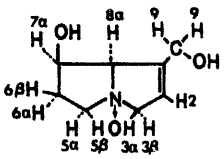

III

δ 1.90–2.30 and δ 2.40–2.84 (both multiplets, both 1H, H6α and H6β), δ 3.55–4.03 (multiplet, 2H, H5α, H5β), δ 4.25 (singlet, 3H, H9, H7α), δ 4.40 (singlet, 1H, H8α), δ 4.50–4.75 (multiplet, 2H, overlapped by the HDO peak at δ 4.80, H3α, H3β), δ 5.81 (multiplet, 1H, H2).

Several differences exist between the spectra of retronecine (at 100 MHz in D_2O; Culvenor et al., 1965) and retronecine N-oxide. The signals due to the protons attached to C3, C5, and C6 are shifted to lower fields, which is consistent with the deshielding effect of a positively charged nitrogen nucleus observed with a number of protonated amines (Ma and Warnhoff, 1965). The signals due to H6α, H6β occur as a single multiplet for retronecine and as separate multiplets for retronecine N-oxide, whereas the reverse is true for H5α, H5β and H6α, H6β. A partial explanation for this effect would be the changes in stereochemistry and anisotropy that could occur when the basic nitrogen is replaced by the N-oxide group. Both the exo-buckled form, which is preferred for retronecine (Culvenor et al., 1965), and the anisotropic effect that is possibly provided by the lone pair of electrons belonging to the bridgehead nitrogen (Jackman and Sternhell, 1969) could be altered by the presence of the N-oxide group. Consequently, changes in deshielding and coupling effects could result. Another difference is the reversed assignment for the H7α and H8α signals in the case of retronecine N-oxide. The H8α proton adjacent to the positively charged nitrogen would be more deshielded than the H7α proton, consequently reversing the assignments. The H7α signal for retronecine is a distinct multiplet whereas the peak at 4.40 ppm is a slightly distorted singlet in the case of retronecine N-oxide.

The carbon-13 spectrum of retronecine N-oxide shows 8 peaks (Table 3) which were assigned by comparison with the values reported for retronecine hydrochloride in D_2O (Mody et al., 1979). Since the nitrogen atoms in both molecules are positively charged, the maximum changes in the two spectra should occur for carbons C3, C5 and C8 which are adjacent to the N-oxide. This change would depend upon the difference between the extent of the positive charge on the protonated and the N-oxide nitrogen atoms. Mody et al. (1979) suggested that the assignments reported for the pyrrolizidine nucleus in europine N-oxide (IV; Zalkow et al., 1978), an ester of an isomer of retronecine N-oxide,

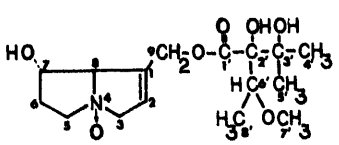

IV

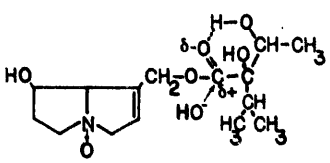

VII

TABLE 3

CARBON-13 SHIFTS AND ASSIGNMENTS FOR RETRONECINE N-OXIDE [a] AND RETRONECINE HYDROCHLORIDE

Carbon	Retronecine N-oxide	Retronecine hydrochloride [b]
1	136.45	135.7
2	120.63	120.5
3	78.58	56.8
5	70.14	53.1
6	34.39	34.2
7	68.83	68.4
8	95.59	77.8
9	58.66	60.5

[a] Isolated from hydrolysis solutions.
[b] Value from Mody et al. (1979).

heliotrine N-oxide (V) might be in error. Our assignments for retronecine N-oxide, which would be expected to be similar to those of the heliotrine N-oxide nucleus, do not agree with those of Zalkow et al. (1978) for carbons C3, C5, C7 and C8. The major fragments resulting from the mass spectral degradation pathways of retronecine N-oxide are shown in Scheme III. In addition to the very low abundant molecular ion at m/e 171, an equally abundant peak is found at m/e 172. Major differences between the mass spectra of retronecine N-oxide and retronecine (Neuner-Jehle et al., 1965) are the presence of

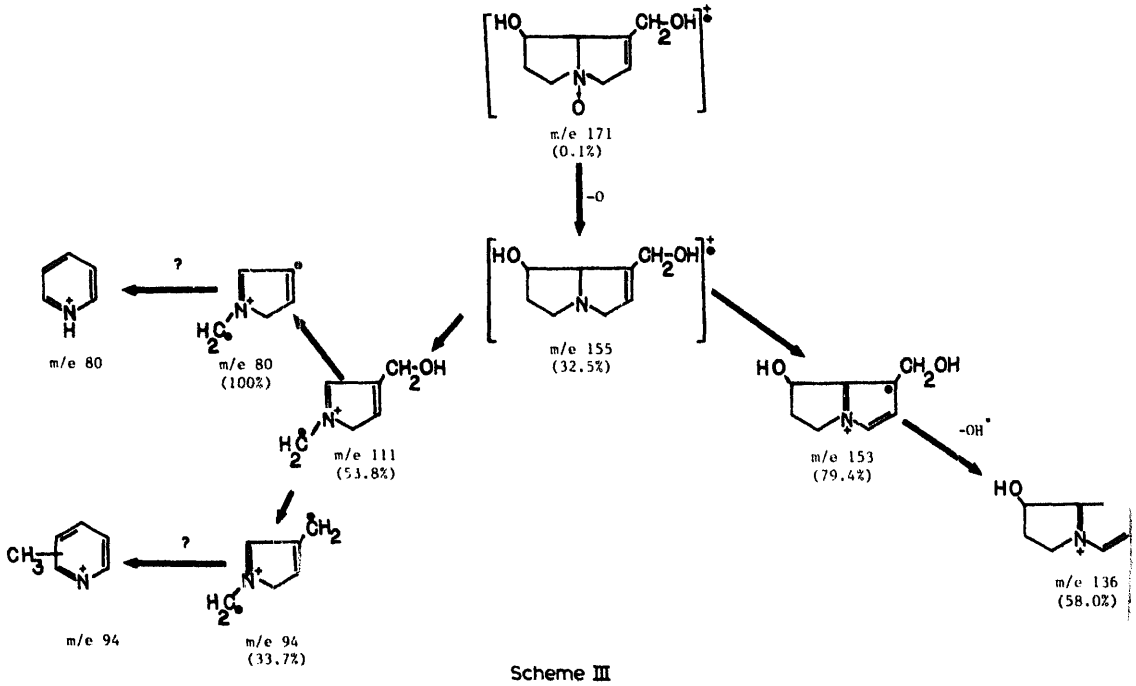

Scheme III

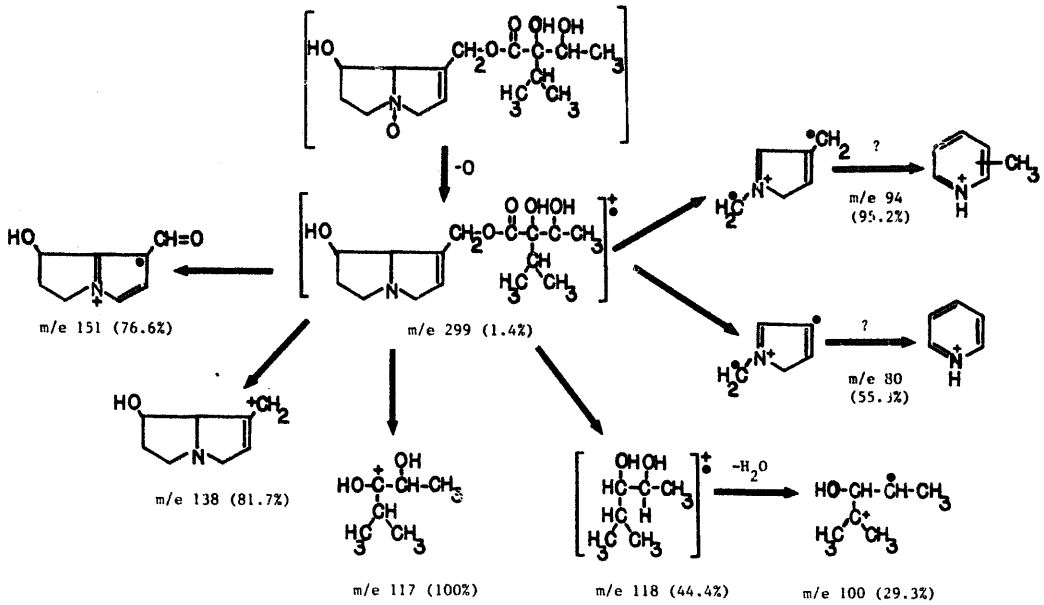

Scheme IV

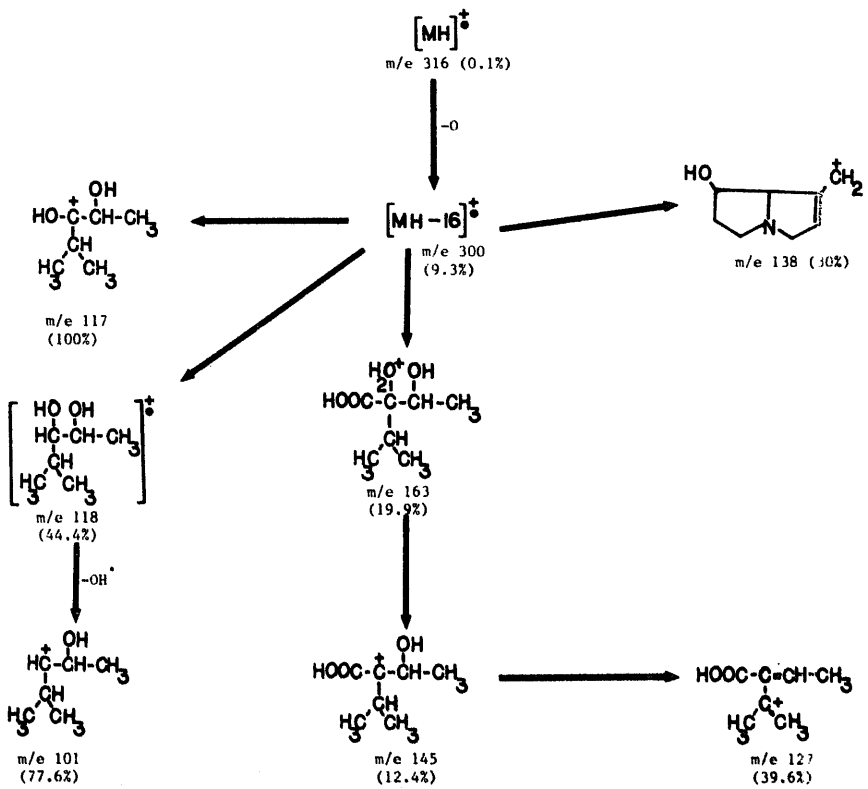

Scheme V

abundant fragments at m/e 153 and 136 for the N-oxide species.

The mass spectrum of indicine N-oxide was recorded under both electron impact and chemical ionization conditions using iso-butane gas. The major degradation fragments are shown in Schemes IV and V. The electron impact mass spectrum of indicine N-oxide reported by Kugelman et al. (1976) lists major fragments at m/e 299, 161, 138, and 117, no molecular ion being observed due to the facile loss of oxygen from the N-oxide. All 4 fragments were observed by us though the m/e 161 fragment had a relative intensity of only 0.3%. Of the observed fragments not previously reported, the fragment at m/e 151 appears structurally similar to that at m/e 153 in our retronecine N-oxide spectra. The cleavage of the ester linkage to produce the aldehydic group in the m/e 151 fragment was also found in the mass spectrum of senecionine, another pyrrolizidine alkaloid ester (Bull et al., 1968). The major differences between the chemical ionization and electron impact mass spectra of indicine N-oxide are the appearance of a low intensity quasi-molecular ion at m/e 316 and an abundant fragment at m/e 163, accompanied by the almost complete dissappearance of the m/e 151, 94, and 80 fragments in the chemical ionization spectra.

Mechanism

Bimolecular acyl-oxygen cleavage is the most common mechanism for the hydrolysis of esters in sodium hydroxide. Data for the hydrolysis of indicine N-oxide in the presence of sodium hydroxide are in agreement with such a mechanism as shown in Scheme VI.

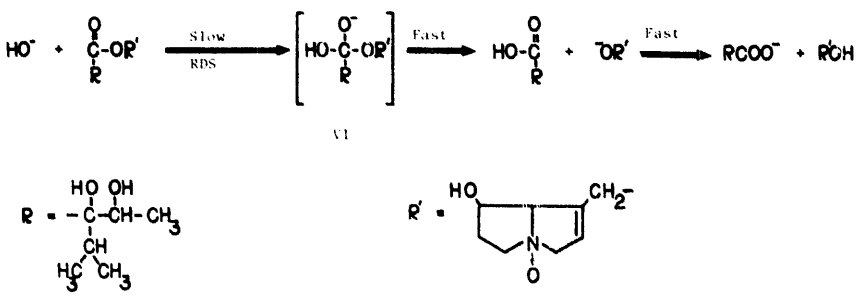

The rate-determining step (RDS) formation of the tetrahedral intermediate (VI) should be facilitated by the proposed intramolecular hydrogen bonding in indicine N-oxide (VII).

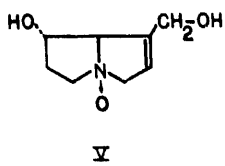

V

The slow rate of hydrolysis of naturally occurring pyrrolizidine alkaloid esters has been attributed to steric hindrance by the branched esterifying acids (Bull et al., 1968). A priori, comparing indicine N-oxide to the unhindered aliphatic ester ethyl acetate (which has a hydrolysis rate 58 times faster at 25°C) one would predict that the activation energy and enthalpy of activation would be nearly equal to or slightly lower than for indicine

N-oxide if intramolecular catalysis is taken into account (VII). To obtain these values, the data from the second-order experiments (Table 2) were treated using the Arrhenius equation:

$$k_2 = Ae^{-E_a/RT} \tag{5}$$

where k_2 is the bimolecular rate-constant, A is the pre-exponential factor, E_a is the energy of activation, R is the gas constant, and T is the absolute temperature. The log transformation of Eqn. 5 is:

$$\ln k_2 = \ln A - \frac{E_a}{RT} \tag{6}$$

Fig. 4 presents the ln k_2 vs 1/T plot for the data in Table 2. The activation energy for the attack of the hydroxide species on the indicine N-oxide molecule, obtained from the slope of the line, is 16.1 kcal/mole. To obtain the enthalpy and entropy of activation, second-order kinetic data (Table 2) were analyzed using the following equation:

$$k_2 = \frac{RT}{Nh}\,[e^{\Delta S^{\ddagger}/R}]\,[e^{-\Delta H^{\ddagger}/RT}] \tag{7}$$

where k_2 is the bimolecular rate-constant, R is the gas constant, T is the absolute temperature, N is Avogadro's number, h is Planck's constant, $\Delta S^{\ddagger}$ is the entropy of activation, and $\Delta H^{\ddagger}$ is the enthalpy of activation. Dividing by T followed by a log transformation

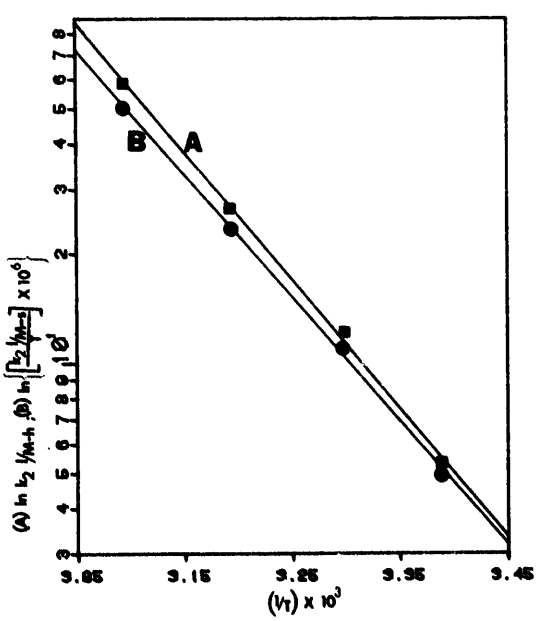

Fig. 4. Semi-ln plots of (A) k_2 vs 1/T (Eqn. 6) and (B) k_2/T vs 1/T (Eqn. 8) where k_2 is the bimolecular rate-constant for the hydrolysis of indicine N-oxide in aqueous sodium hydroxide (Table 2).

gives:

$$\ln(k_2/T) = \left(\ln\frac{R}{Nh}\right) + \frac{\Delta S^{\ddagger}}{R} - \frac{\Delta H^{\ddagger}}{RT} \tag{8}$$

Fig. 4 also shows the $\ln(k_2/T)$ vs $1/T$ plot for the data in Table 2. The value of $\Delta H^{\ddagger}$ obtained from the slope of the line is 15.5 kcal/mole-deg., and that of $\Delta S^{\ddagger}$ obtained from the intercept is −18.8 e.u.

Hydrolysis of ethyl acetate in aqueous sodium hydroxide has been reported by Halonen (1956) and Pan et al. (1962). The average activation energy was 11.45 (±0.35) kcal/mole. The data on Halonen (1956) were analyzed using Eqns. 7 and 8 to obtain values for $\Delta H^{\ddagger}$ and $\Delta S^{\ddagger}$ which were averaged with the values reported by Pan et al. (1965), to obtain an average $\Delta H^{\ddagger}$ of 10.85 (±0.35) kcal/mole and $\Delta S^{\ddagger}$ of −26.55 (±1.25) e.u. The slower hydrolysis rate of indicine N-oxide is therefore associated with its higher energy of activation. Inductive effects do not appear to play a prominent role. By employing the substituent constants reported by Charton (1964) the calculated inductive potential of the tranchelanthic acid side-chain is negligible since the negative hydroxyl effects if offset by the contribution of the alkyl groups, steric hindrance appears to be the prime reason for the reduced hydrolysis rate and increased E_a value. An increase in the E_a values for the alkaline hydrolysis of several aliphatic esters with aryl and alkyl substitutions in the acyl part has been attributed to steric hindrance (Levenson and Smith, 1940a and b). The alkaline stability of ethyl diisopropylacetate and ethyl dicyclopentylacetate (Von Braun and Fischer, 1933) illustrate just how effective steric factors can be. The rule of 6 (Newman, 1950) states that atoms separated from the attacking species in the transition state by a chain of 4 atoms provide the greatest steric hindrance. In the case of ethyl di-isopropylacetate and ethyl dicyclopentylacetate there are 12 and 8 hydrogen atoms

TABLE 4

HALF-LIFE VALUES ($t_{0.5}$) FOR HYDROLYSIS OF PYRROLIZIDINE ALKALOID ESTERS IN 0.5 N NaOH AT 25°C.

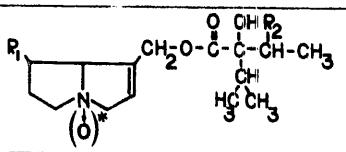

	R_1	R_2	Medium	$t_{0.5}$
Alkaloids				
Supinine [a]	H	OH	50% aqueous ethanol	100 min
Heleurine [a]	H	OCH_3	50% aqueous ethanol	20 days
N-oxides *				
Indicine N-oxide [b]	OH	OH	water	13 min
Heliotrine N-oxide [a]	OH	OCH_3	water	2 days

[a] Reported by Bull et al. (1968).
[b] Determined in this study.

respectively. Indicine N-oxide has 10 hydrogen atoms in the trachelanthic acid portion that can cause maximum steric hindrance according to this rule.

The higher value of $\Delta S^{\ddagger}$ for indicine N-oxide is probably an anomoly and is found in other cases as well. The hydrolysis of ethyl diphenylacetate when compared to that of ethyl phenylacetate would be expected to result in a lower value of $\Delta H^{\ddagger}$ due to the negative inductive effect of the second phenyl group and a lower $\Delta S^{\ddagger}$ value due to additional steric hindrance. The data for the alkaline hydrolysis of the two species in aqueous ethanol reported by Levenson and Smith (1940b) were analyzed using Eqns. 7 and 8 to obtain values of $\Delta H^{\ddagger}$ = 13.4 kcal/mole and 15.4 kcal/mole for ethyl phenylacetate and ethyl diphenylacetate, respectively. The corresponding values of $\Delta S^{\ddagger}$ are −8.91 e.u. and −7.91 e.u. Thus, steric hindrance again is reflected by the value of $\Delta H^{\ddagger}$ rather than $\Delta S^{\ddagger}$.

The hydrolysis data for 4 pyrrolizidine alkaloid esters listed in Table 4 reconfirms the acceleration of the rate by the β-hydroxyl group. This has previously been attributed to hydrogen bonding between the β-hydroxyl and the carbonyl group (VIII; Bull et al., 1968). It also appears that the presence of the hydroxyl group (R_2) increases the hydrolysis rate by a factor of approximately 200.

ACKNOWLEDGEMENTS

Supported in part by National Cancer Institute, Contract CM-87161, Division of Cancer Treatment, and Grant CA-16058 from the National Cancer Institute, National Institutes of Health.

The authors are grateful to the Drug Synthesis and Chemistry Branch, Division of Cancer Treatment, National Cancer Institute, for supplying indicine N-oxide and to Louis Malspeis for his assistance.

REFERENCES

Adams, R. and Van Duuren, B.L., Trachelanthic and viridifloric acids. J. Am. Chem. Soc., 74 (1952) 5349–5351.

Ames, M.M. and Powis, G., Determination of indicine N-oxide and indicine in plasma and urine by electron-capture gas–liquid chromatography. J. Chromatogr., 166 (1978) 519–526.

Bull, L.B., Culvenor, C.C.J. and Dick, A.T., The Pyrrolizidine Alkaloids, North-Holland, Amsterdam, The Netherlands, 1968, pp. 32, 61, 57.

Charton, M., Definition of "inductive" substituent constants. J. Org. Chem., 29 (1964) 1222–1227.

Culvenor, C.C.J., Tumor-inhibitory activity of pyrrolizidine alkaloids. J. Pharm. Sci., 57 (1968) 1112–1117.

Culvenor, C.C.J., Heffernan, M.L. and Woods, W.G., Nuclear magnetic resonance spectra of pyrrolizidine alkaloids. Austr. J. Chem., 18 (1965) 1605–1624.

D'Silva, J.B. and Notari, R.E., Stability-indicating colorimetric assay for indicine N-oxide using TLC. J. Pharm. Sci., 69 (1980) 471–472.

Halonen, E.A., Activation energies in the alkaline hydrolysis of saturated aliphatic esters. Acta Chem. Scand., 10 (1956) 485–486.

Harned, H.S. and Cook, M.A., The activity and osmotic coefficients of some hydroxide–chloride mixtures in aqueous solution. J. Am. Chem. Soc., 59 (1937) 1890–1893.

Harned, H.S. and Owen, B.B., The Physical Chemistry of Electrolytic Solutions, Reinhold, New York, 1958, p. 729.

Jackman, L.M. and Sternhell, S., Applications of Nuclear Magnetic Resonance Spectroscopy in Organic Chemistry, Pergamon Press, England, 1969, p. 81–82.

Kochetkov, N.K., Likhosherstov, A.M. and Kulakov, V.N., The total synthesis of some pyrrolizidine alkaloids and their absolute configuration. Tetrahedron, 25 (1969) 2313–2323.

Kugelman, M., Liu, W.C., Axelrod, M., McBride, T.J. and Rao, K.V., Indicine N-oxide: The antitumor principle of *Heliotropium indicum*. Lloydia, 39 (1976) 125–128.

Kupchan, M.S. and Suffness, M.I., Tumor inhibitors XXII. Senecionine and senecionine N-oxide of *Senecio triangularis*. J. Pharm. Sci., 56 (1967) 541–543.

Levenson, H.S. and Smith, H.A., The saponification of ethyl esters of aliphatic acids. J. Am. Chem. Soc., 62 (1940a), 1556–1558.

Levenson, H.S. and Smith, H.A., Kinetics of the saponification on the ethyl esters of several phenyl-substituted aliphatic acids. J. Am. Chem. Soc., 62 (1940b) 2324–2327.

McComish, M., Bodek, I. and Branfman, A.R., Quantitation of the antineoplastic agent indicine N-oxide in human plasma by differential pulse polarography. J. Pharm. Sci., 69 (1980) 727–729.

Ma, J.C.N. and Warnhoff, E.W., On the use of nuclear magnetic resonance for the detection, estimation, and characterization of N-methyl groups. Can. J. Chem., 43 (1965) 1849–1869.

Mattocks, A.R., Spectrophotometric determination of unsaturated pyrrolizidine alkaloids. Anal. Chem., 67 (1967) 443–447.

Mattocks, A.R., Schoental, R., Crowley, H.C. and Culvenor, C.C.J., Indicine: the major alkaloid of *Heliotropium indicum L.* J. Chem. Soc., (1961) 5400–5403.

Mody, N.V., Sawhney, R.S. and Pelletier, S.W., Carbon-13 nuclear magnetic resonance spectral assignments for pyrrolizidine alkaloids, J. Nat. Prod., 42 (1979) 417–420.

Neuner-Jehle, N., Nesvadba, H. und Spiteller, G., Anwendung der massenspektrometrie Zur struktuaufklärung von alkaloiden, 6. Mit: Pyrrolizidinalkaloide aus dem Goldregen. Montash. Chem. 96 (1965) 321–338.

Newman, M.S., Some observations concerning steric factors. J. Am. Chem. Soc., 72 (1950) 4783–4786.

Pan, K., Chang, C.F. and Hong, H.S., Kinetic studies of the alkaline hydrolysis of alkyl acetates by conductometric measurements. J. Chinese Chem. Soc., Ser. II, 9 (1962) 89–99.

Von Braun, J. und Fischer, F., Beiträge zur kenntnis der sterischen Hinderung, VII Mitteil.: Veresterung und Verseifung vom standpunkt der elektronischen Theorie der Bindung. Ber., 66 (1933) 101–104.

Zalkow, L.H., Gelbaum, L. and Kleinan, E., Isolation of the pyrrolizidine alkaloid europine N-oxide from *Heliotropium maris-mortui* and *H. rotundifolium*. Phytochemistry, 17 (1978) 172.